CHEMMEDCHEM

DOI: 10.1002/cmdc.201000124

Novel Monocyclam Derivatives as HIV Entry Inhibitors: Design, Synthesis, Anti-HIV Evaluation, and Their Interaction with the CXCR4 Co-receptor

Sofia Pettersson,[a] Violeta I. Pérez-Nueno,[a] Maria Pau Mena,[b] Bonaventura Clotet,[b] José A. Esté,[b] José I. Borrell,*[a] and Jordi Teixidó[a, c]

The CXCR4 receptor has been shown to interact with the human immunodeficiency virus (HIV) envelope glycoprotein gp120, leading to fusion of viral and cell membranes. Therefore, ligands that can attach to this receptor represent an important class of therapeutic agents against HIV, thus inhibiting the first step in the cycle of viral infection: the virus–cell entry/fusion. Herein we describe the in silico design, synthesis, and biological evaluation of novel monocyclam derivatives as HIV entry inhibitors. In vitro activity testing of these compounds in cell cultures against HIV strains revealed EC_{50} values in the low micromolar range without cytotoxicity at the concentrations tested. Docking and molecular dynamics simulations were performed to predict the binding interactions between CXCR4 and the novel monocyclam derivatives. A binding mode of these compounds is proposed which is consistent with the main existing site-directed mutagenesis data on the CXCR4 co-receptor. Moreover, molecular modeling comparisons were performed between these novel monocyclams, previously reported non-cyclam compounds from which the monocyclams are derived, and the well-known AMD3100 bicyclam CXCR4 inhibitors. Our results suggest that these three structurally diverse CXCR4 inhibitors bind to overlapping but not identical amino acid residues in the transmembrane regions of the receptor.

Introduction

According to the Joint United Nations Programme on HIV/AIDS (UNAIDS) and World Health Organization (WHO), a total of 33.2 million [30.6–36.1 million] people were living with human immunodeficiency virus (HIV) in 2007.[1] Studies in HIV biology have provided deep knowledge of the molecular events involved in the HIV life cycle, which consist of several steps: viral entry, reverse transcription, integration, gene expression, gene assembly, budding and maturation.[2–4] Current antiretroviral therapies (ARTs) against HIV are generally based on the combination of reverse transcriptase and protease inhibitors which is known as highly active antiretroviral therapy (HAART). At the present time there are nucleoside and non-nucleoside reverse transcriptase inhibitors (NRTI, NNRTI), protease inhibitors (PI), a fusion inhibitor, an entry inhibitor and an integrase inhibitor available for the treatment of HIV infection.[5] Despite the large number of drugs available, there are several concerns about antiretroviral regimens. The drugs can have serious side effects, regimens can be complicated requiring patients to take several pills at various times during the day, drug resistance, latent viral reservoirs and drug induced toxic effects that compromise effective viral control can be developed. Fusion/entry inhibitors have been shown to be effective in patients harboring resistance to the NRTI, NNRTI, and PI classes.[6] Therefore, there is considerable interest in developing novel ligands that are resistant to the currently used drugs or new agents belonging to new classes that further heighten the effectiveness and durability of HIV therapy.[7,8]

Bicyclams were the first low molecular weight compounds with a specific interaction with CXCR4.[9–12] The most potent bicyclam was AMD3100 ($EC_{50} = 0.001\ \mu g\,mL^{-1}$) in which the two cyclam moieties are tethered by a 1,4-phenylenebis(methylene) bridge. However, AMD3100 has been shown to exhibit poor oral absorption and toxicity, which are related to its high positive charge at physiological pH. To improve these characteristics, analogous compounds with fewer basic amine groups have been developed, such as monocyclam derivatives (AMD3465 and AMD3451) and non-cyclam derivatives (AMD070 and **1**) (Figure 1).[13–15]

Results and Discussion

Rational design of monocyclam derivatives

It has been proven that the eight amino groups present in AMD3100 are not essential for the interaction with the CXCR4 co-receptor.[13,16] Furthermore, previous work in our group led

[a] *Dr. S. Pettersson, Dr. V. I. Pérez-Nueno, Dr. J. I. Borrell, Dr. J. Teixidó*
Grup d'Enginyeria Molecular, Institut Químic de Sarrià
Universitat Ramon Llull, Via Augusta 390, 08017 Barcelona (Spain)
Fax: (+34) 932 056 266
E-mail: jose.borrell@iqs.url.edu

[b] *Dr. M. P. Mena, Dr. B. Clotet, Dr. J. A. Esté*
Retrovirology Laboratory IrsiCaixa
Hospital Universitari Germans Trias i Pujol
Universitat Autònoma de Barcelona, 08916 Badalona (Spain)

[c] *Dr. J. Teixidó*
Current address: Mataró-Maresme TecnoCampus Foundation
Edifici TecnoCampus v. 1.0, Vallveric
85 1a Planta Local 3i5, 08304 Mataró Barcelona (Spain)

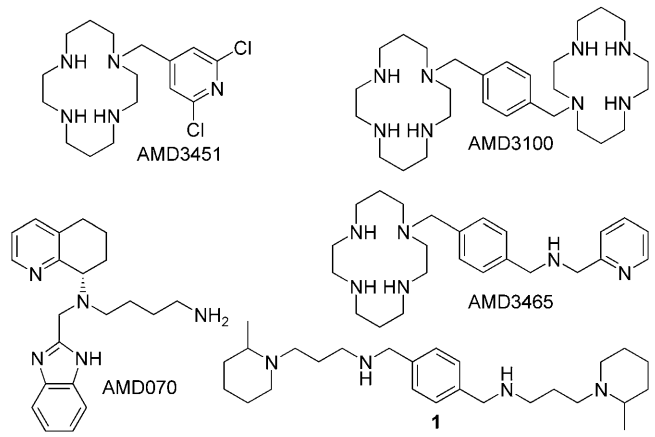

Figure 1. Structure of bicyclam AMD3100, monocyclams AMD3451 and AMD3465, and non-cyclam CXCR4 inhibitors AMD070 and **1**.

to the discovery of a series of non-cyclam CXCR4 inhibitors with **1** being the most active thereof, with only four nitrogen atoms.[17] Based on this evidence, we designed a library of new monocyclam derivatives which combine the cyclam ring with the diamines used in our previous work.[17] A selection of the presumably most active compounds (**2** and **3**) was accomplished with published virtual screening methods.[18] Here, we report on the synthesis, binding mode studies and anti-HIV activity of these two novel monocyclam derivatives.

Chemistry

Described synthetic procedures for monocyclam derivatives use the alkylation of an amine, generally a secondary amine, with a brominated cyclam derivative (compound **4**).[19] However, the use of **4** in the alkylation of primary amines **6** and **7** did not lead to the target monocyclam derivatives **2** and **3** due to polyalkylation side reactions. Therefore, we designed a new synthetic strategy to obtain the target substituted monocyclams. The retrosynthetic analysis of these compounds afforded the corresponding primary amine and a novel key intermediate, the aldehyde derivative **5** (Figure 2). This compound can be obtained in high yield by alkylation of the non-protected amino group in **12** with **10** in the presence of potassium carbonate (Scheme 1). These two precursors were obtained by previously reported methods. Compound **12** was synthesized by the N1-Boc protection of cyclam **11**.[20] Bromoaldehyde **10** was achieved by reduction of the aldehyde **8** with sodium borohydride in methanol followed by deprotection of the latent formyl group in hydrochloric acid and bromination with NBS and triphenylphosphine.[21] Finally a stepwise reductive amination of the key intermediate **5** with the corresponding primary amines **6** and **7** followed by cleavage of the *tert*-butyl carbamates in acidic conditions afforded monocyclams **2** and **3** (Scheme 1).

Biological evaluation

We determined the anti-HIV activity of these novel monocyclams and compared it with the values obtained for the known CXCR4 inhibitors AMD3465 and **1**. EC_{50} values of monocyclams **2** and **3** were 0.02 and 0.06 $\mu g\,mL^{-1}$, respectively

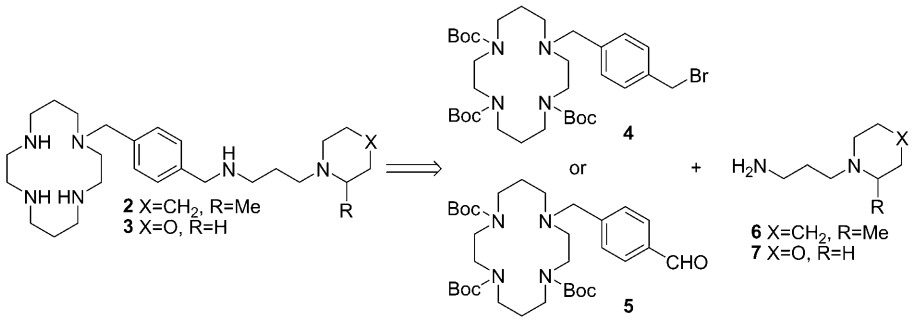

Figure 2. Scheme showing the building blocks for synthesis of monocyclams **2** and **3**: brominated derivative **4** or aldehyde **5** and the corresponding amine **6** or **7**.

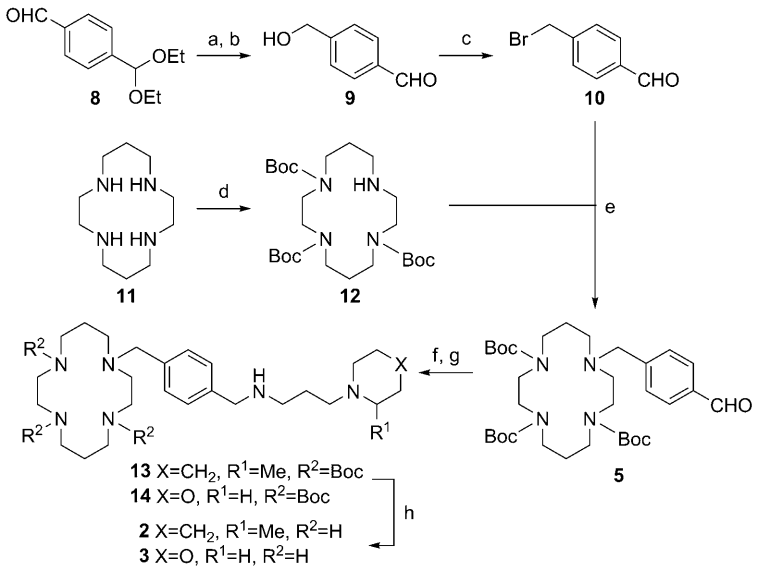

Scheme 1. Synthetic route for monocyclam derivatives **2** and **3**. Reagents and conditions: a) $NaBH_4$, MeOH, room temperature, 6 h; b) HCl/H_2O, room temperature, 2 h; c) NBS, PPh_3, CH_2Cl_2, reflux, 2 h; d) Boc_2O, CH_2Cl_2, reflux, 6.5 h; e) K_2CO_3, MeCN, reflux, 16 h; f) **6**, $Ti(OiPr)_4$, EtOH, room temperature, 36 h, or **7**, MeOH, MW, 100 °C, 3 h; g) $NaBH_4$, room temperature, 12 h; h) HCl/Et_2O, room temperature, 12 h.

Table 1. Anti-HIV activity, cytotoxicity, and Gibbs free energy of selected hits.

Compd	EC_{50} [$\mu g\,mL^{-1}$][a]	CC_{50} [$\mu g\,mL^{-1}$][b]	ΔG_{exp} [$kcal\,mol^{-1}$][c]	ΔG_{calcd} [$kcal\,mol^{-1}$][d]
1	0.008 ± 0.001	>25	-10.5	-10.6
2	0.02 ± 0.006	>25	-10.3	-9.7
3	0.06 ± 0.005	>25	-9.7	-9.9
AMD3465[50]	0.004	>25	-11.0	-11.4

[a] Concentration required to inhibit HIV-1-induced cell death by 50% as evaluated with the MTT method in MT-4 cells; values represent the mean $\pm$SD of at least two independent evaluations done in triplicate. [b] Concentration required to induce 50% death of non-infected MT-4 cells as evaluated with the MTT method. [c] Experimental Gibbs free energy computed as $\Delta G \approx RT\ln(EC_{50})$;[51] $R = 0.001988$, $T = 298.15$ K. [d] Theoretical Gibbs free energy obtained from the AutoDock Vina docking affinity.[52]

(Table 1). These compounds showed potent antiviral activity, but are 10-fold less active than **1** and AMD3465. We expected higher antiviral because they combine the best from each family, a cyclam moiety (from AMD3100) and a pipecoline (from compound **1**). Therefore we performed theoretical binding mode studies that we describe herein.

To verify the specificity of **1**–**3** for CXCR4, their capacity to interfere with the staining of monoclonal antibodies (mAbs) against CXCR4, CD45 (control receptor), or CD4 (HIV receptor) was tested. MT-4 cells were stained with mAbs alone or together with study compounds or control compounds with known epitope specificities. Compounds **1**, **2**, and **3** inhibited the staining of CXCR4 on cells with mAb 12G5-PE in a dose-dependent manner, with IC_{50} values of 0.06, 0.03, and 0.11 $\mu g\,mL^{-1}$, respectively (Figure 3a and 3b). The staining of CXCR4 was also inhibited by the CXCR4 antagonist AMD3100 with an IC_{50} value of 0.02 $\mu g\,mL^{-1}$ and by the unstained 12G5 antibody ($IC_{50} = 14.7$ $\mu g\,mL^{-1}$). Conversely, AMD3100, **1**, **2**, and **3** did not interfere with the staining using mAbs specific for CD45 or CD4 (Figure 3b). Taken together, these results suggest that compounds **1**–**3** are specific antagonists of CXCR4.

Theoretical binding mode studies: docking and molecular dynamics refinement

A theoretical binding mode study was performed in order to predict the binding interactions of the synthesized monocyclams with the CXCR4 receptor pocket. Compounds **2** and **3** were docked onto the site-directed mutagenesis (SDM)-defined CXCR4 binding pocket[16,22–30] using AutoDock Vina.[31,32] The highest-affinity binding modes obtained are shown in Figure 4a and 4b, respectively. These affinities are listed in Table 1, as well as how they correlate with antiviral activities. The Gibbs free energy (ΔG) is used to compare theoretical and experimental activities. The key SDM residues for monocyclam, non-cyclam, and bicyclam interactions[16,30] are shown as orange sticks. Ligand interactions were analyzed in MOE[33] using hydrogen bond, ionic, and solvent contacts with a minimum qualifying score of 5%, and non-bonded contacts within a maximum distance of 4.5 Å. In the high-affinity binding conformation of **2**, a backbone hydrogen bond donor was found between the protonated pipecoline and the Tyr7 oxygen and non-bonded interactions were found between the ligand and Ile6, Tyr7, Thr8, Ser9, Phe36, Leu41, Ala95, Ala98, Phe104, Gly105, Asn106, Val112, Tyr190, Asp262,

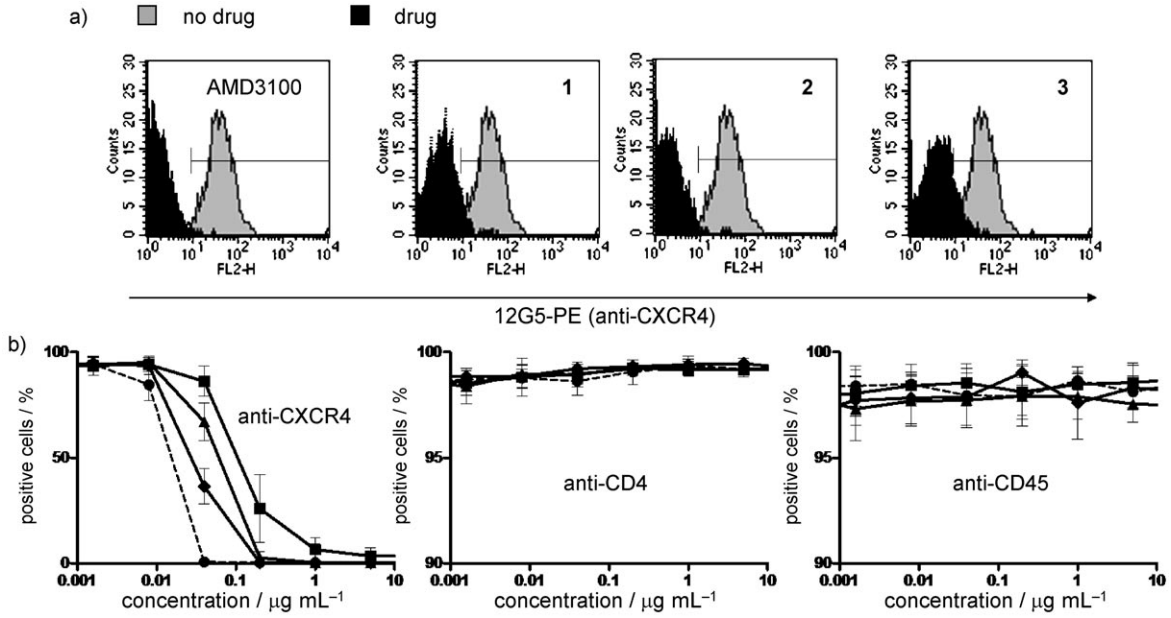

Figure 3. a) Inhibition of mAb 12G5-PE (anti-CXCR4) staining on MT-4 cells by various compounds (CXCR4 antagonist AMD3100 at 0.04 $\mu g\,mL^{-1}$, **1** at 0.2 $\mu g\,mL^{-1}$, **2** at 0.2 $\mu g\,mL^{-1}$, and **3** at 1 $\mu g\,mL^{-1}$); the marker was defined as 1% of the control isotype. b) Dose–response curves of the inhibition of staining with mAb anti-CXCR4 12G5-PE by the CXCR4 antagonist AMD3100 (●), **1** (▲), **2** (◆), and **3** (■). Staining with anti-CD4 and anti-CD45 was not inhibited by the compounds; data represent the mean $\pm$SD of three independent experiments.

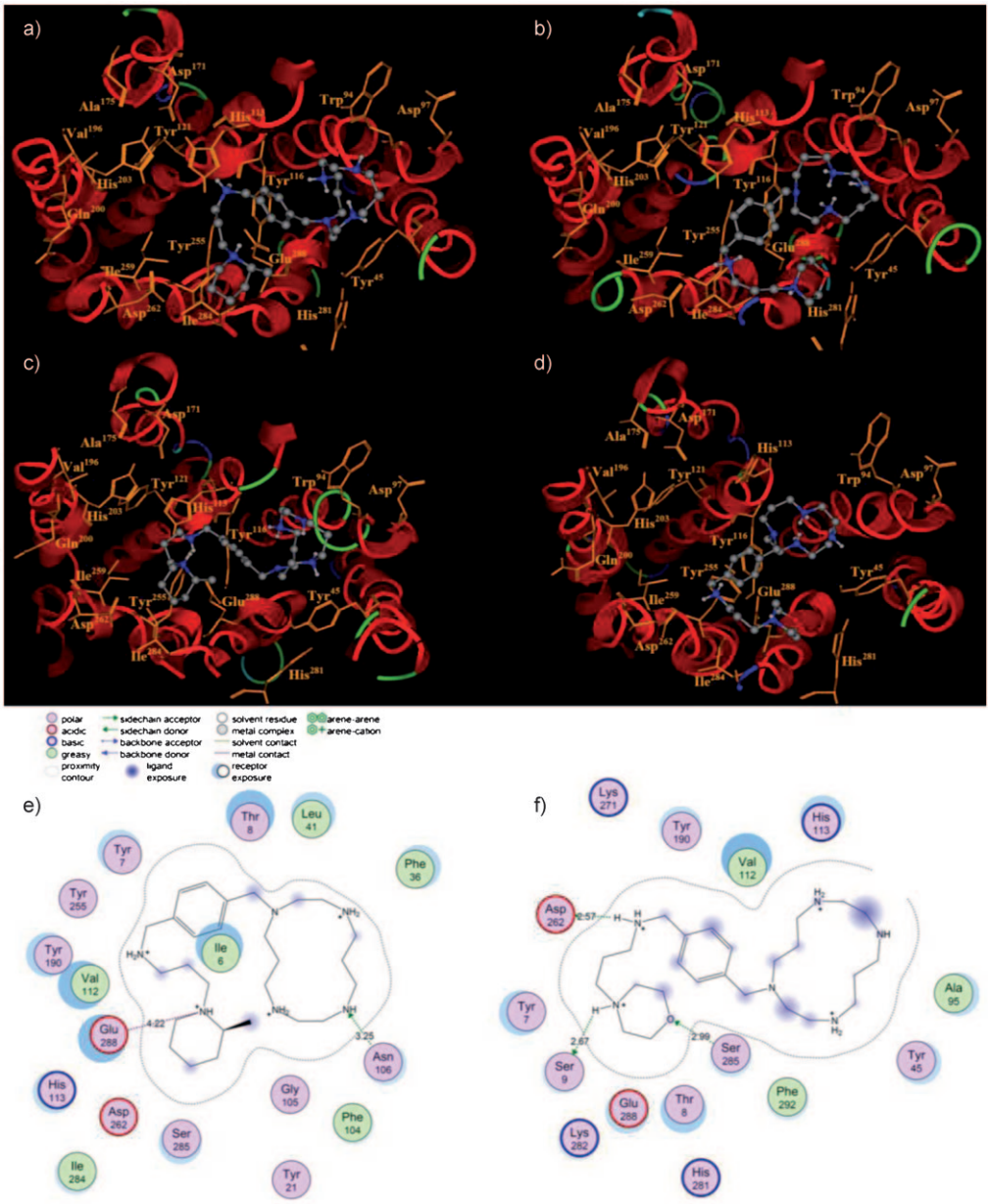

Figure 4. Potential binding modes of **2** and **3**. At top, the highest-affinity binding conformations for a) **2**–CXCR4 and b) **3**–CXCR4 obtained by docking with AutoDock Vina. c) **2**–CXCR4 and d) **3**–CXCR4 binding modes obtained by MD simulations using Amber 8. For clarity, all the intracellular and extracellular loops are omitted, and only polar hydrogen atoms are shown in structures. The key CXCR4 SDM residues are shown as orange sticks. At the bottom, 2D diagram of the e) CXCR4–**2** and f) CXCR4–**3** ligand interactions found for the MD binding modes obtained. The diagram depicts the hydrogen bond, ionic, solvent and non-bonded contacts. Contact distances are also labeled. The CXCR4 SDM residues (Glu288, Asp262, His281, Tyr 45) with the highest level of the effect of the mutation on the binding of monocyclam compounds (such as AMD3465, AMD8721, AMD8899, AMD3529 and AMD3389) appear in the binding modes obtained. Other CXCR4 SDM residues (His113, Tyr255, Ile284) with lower levels of the effect of the mutation on the binding of monocyclam compounds also take part in the binding conformations calculated.

Trp283, Tyr284, Ser285, Glu288 and Phe292. On the other hand, the high-affinity binding conformation of **3** showed two ionic interactions between the non-cyclam protonated secondary amine and the Asp262 oxygen and the cyclam ring protonated N4 and the Glu288 oxygen, respectively. Also, non-bonded interactions were found between the ligand and Ile6, Tyr7, Thr8, Ser9, Glu31, Phe36, Leu41, Ala95, Asn106, Val112, Tyr190, Asp262, His281, Lys282, Trp283, Tyr284, Ser285, Glu288 and Phe292. Docking results agree with some of the CXCR4 SDM residues with the highest level of the effect of the mutation on the binding of monocyclam compounds,[16] such as AMD3465, AMD3529 (both having quite similar structures to our monocyclam designed compounds), AMD8721, AMD8899 or AMD3389. These compounds seem to interact especially with Glu288, Asp262, and His281, which are interactions that also appear in our monocyclam designed compounds.

These high-affinity docked poses obtained were used as the starting structures for molecular dynamics (MD) refinement

using Amber 8.[34] The binding modes obtained are shown in Figure 4c and 4d, respectively. The ligand interactions were also analyzed in MOE using the same parameters. They are shown in Figure 4e and 4f, respectively. In the binding conformation of **2** a side chain hydrogen bond acceptor was found between the cyclam ring N8 and the Asn106 amino group, an ionic interaction was found between the pipecoline protonated nitrogen and the Glu288 oxygen and non-bonded interactions were found between the ligand and Ile6, Tyr7, Thr8, Tyr21, Phe36, Leu41, Phe104, Gly105, Asn106, Val112, His113, Tyr190, Asp262, Tyr284, Ser285 and Glu288. In the binding conformation of **3**, two side chain hydrogen bond donors were found between the morpholine protonated nitrogen and the Ser9 oxygen and the non-cyclam protonated secondary amine and the Asp262 oxygen, a side chain hydrogen bond acceptor was found between the morpholine oxygen and the Ser285 hydroxy group. Non-bonded interactions were found between the ligand and Tyr7, Thr8, Ser9, Tyr45, Ala95, Val112, His113, Tyr190, Asp262, Lys271, His281, Lys282, Ser285, Glu288, and Phe292.

As for the high-affinity docked conformations, the MD refinement results agree with some of the CXCR4 SDM residues with the highest level of the effect of the mutation on the binding of monocyclam compounds (Glu288, Asp262, His281, Trp94, Tyr 45, Tyr116, Asp171) and also other SDM residues with lower levels of the effect of the mutation on the binding of monocyclam compounds (Ala175, His113, Glu200, Tyr255, Ile259, His203, Val196, Ile284, and Tyr121, listed from the upper to lower level).[16,30] The binding conformations obtained are also consistent with one of the three binding modes proposed for monocyclam AMD3465 by Wong et al.,[30] in which there is an aromatic interaction between His281 and the pyridine ring, Glu288 makes an ionic interaction with the protonated dibenzylamine, and the double protonated cyclam ring interacts with Asp262. However, the binding modes obtained cannot account for all of the amino acid residues that have been shown to affect the binding of monocyclam inhibitors in SDM studies.

In general, compounds **2** and **3** appear to mimic the general binding mode of AMD3100, but in a mode where the non-cyclam part picks up novel interactions especially with residues located more toward the extracellular end of transmembrane (TM)-VI and TM-VII (Asp262, Glu288, His281, Tyr255, Ile259, Ile284), making essential interactions at each end of the main ligand binding pocket of the CXCR4 receptor.

Comparison of the theoretical binding modes of bicyclam, monocyclam, and non-cyclam CXCR4 inhibitors

The binding modes of **2** and **3** were compared with the binding modes of other reported monocyclams (AMD3465, AMD3451), the bicyclam AMD3100 and non-cyclams **1** (previously reported by our group and from which **2** is derived), and AMD070. Docking results are shown in Figure 5a. The ligand interactions for the high-affinity binding conformations obtained for **2** and **3** have been described in detail previously. In the case of AMD3465, the high-affinity binding conformation showed a backbone hydrogen bond donor between the non-cyclam protonated secondary amine and Tyr7 oxygen, a side chain hydrogen bond acceptor between the piperidine nitrogen and Ser9 hydroxy group and two ionic interactions between the non-cyclam protonated secondary amine and Asp262 oxygen and the cyclam ring protonated N11 and Glu288 oxygen, respectively. Non-bonded interactions were found between AMD3465 and Ile6, Tyr7, Thr8, Ser9, Leu41, Tyr45, Ala95, Ala98, Asn106, Val112, Tyr190, Lys282, Trp283, Ile284, Ser285, Glu288 and Phe292. The high-affinity binding conformation of AMD3451 showed an ionic interaction between the cyclam ring protonated N11 and Glu288. Non-bonded interactions were found between AMD3451 and Glu2, Ile6, Tyr7, Thr8, Ser9, Phe36, Leu41, Ala98, Phe104, Gly105, Asn106, Val112, Tyr190, Asp262, Lys271, Lys282, Trp283, Ile284, Ser285 and Glu288. In the high-affinity binding conformation of AMD3100, two ionic interactions were found between the cyclam ring protonated N11 and Asp262 oxygens. Non-bonded interactions were found between AMD3100 and Ile6, Tyr7, Thr8, Ser9, Cys109, Val112, His113, Asn176, Arg188, Tyr190, Ile284, Ser285 and Glu288. In the case of **1**, the high-affinity binding conformation showed a side chain hydrogen bond donor between the non-cyclam protonated secondary amine and Ser285 oxygen. Two ionic interactions were found, one between the non-cyclam protonated secondary amine and the Glu288 oxygen and the other between the pipecoline protonated nitrogen and the other Glu288 oxygen. Non-bonded interactions were found between **1** and Glu2, Ile6, Tyr7, Thr8, Phe36, Leu41, Ala95, Ala98, Asn106, Val112, His113, Tyr190, Tyr255, Ile284, Ser285, Glu288 and Phe292. Finally, the high-affinity binding conformation of AMD070 showed three side chain hydrogen bond donors: between the protonated primary amine and Tyr255 oxygen, the protonated primary amine and one Glu288 oxygen and the benzimidazole NH and the other Glu288 oxygen. AMD070 also showed a side chain hydrogen bond acceptor between the benzimidazole NH and the Ser285 hydroxy group and two ionic interactions between the protonated tertiary amine and both Glu288 oxygen atoms, respectively. Non-bonded interactions were found between AMD070 and Tyr7, Thr8, Phe36, Leu41, Tyr45, Val112, His113, Tyr190, Tyr255, Lys282, Ile284, Ser285, Glu288 and Phe292.

Notably, all these molecules interact with overlapping but not identical residues in the binding pocket of the receptor. Depending on the compound structures (monocyclam, bicyclam, or non-cyclam), their interaction with the key CXCR4 SDM residues can vary. However the main interactions seem to be conserved for monocyclams (Asp262, His281, Glu288), non-cyclams (Glu288) and bicyclams (Glu288). In this way, some key SDM residues (Asp262, His281, Ala175, Ile259, Ile284) seem to affect the binding of monocyclams at a higher level than they do for non-cyclams or bicyclams.[16,30]

MD-refined binding poses were compared for monocyclams **2**, **3**, non-cyclam **1**, and the bicyclam AMD3100. They are shown in Figure 5b. Ligand interactions were analyzed in MOE. Figure 5c, 5d, and 5e compare the ligand interactions of a monocyclam (compound **3**), non-cyclam (compound **1**) and bicyclam (AMD3100), respectively. In the binding conformation of **3**, two side chain hydrogen bond donors were found be-

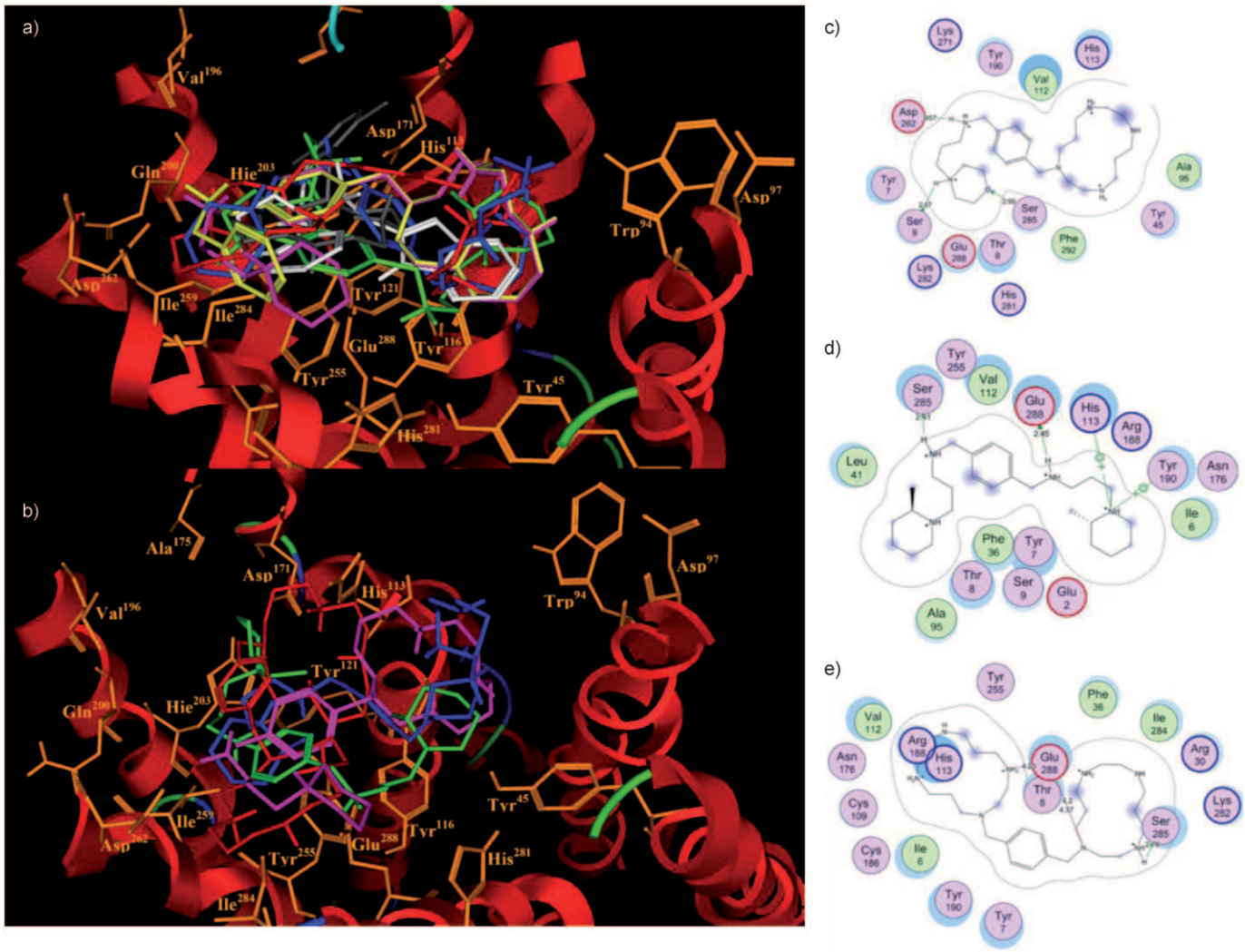

Figure 5. Comparison of the theoretical binding modes of bicyclam, monocyclam and non-cyclam CXCR4 inhibitors. a) Highest-affinity docking poses for monocyclams **2** (blue), **3** (pink), AMD3465 (yellow), and AMD3451 (gray), non-cyclams **1** (green) and AMD070 (white), and bicyclam AMD3100 (red) obtained using AutoDock Vina. b) MD binding poses for monocyclams **2** (blue) and **3** (pink), non-cyclam **1** (green) and bicyclam AMD3100 (red) obtained using Amber 8. At right, ligand interaction 2D diagram comparing the c) monocyclam **3**, d) non-cyclam **1**, and e) bicyclam AMD3100 interactions found. Hydrogen bonds and ionic interactions are shown in green and purple dots, respectively. Interaction distances are also labeled. The legend for the diagrams is the same as shown in Figure 4e.

tween the morpholine protonated nitrogen and the Ser9 oxygen, the non-cyclam protonated secondary amine and the Asp262 oxygen. A side chain hydrogen bond acceptor was found between the morpholine oxygen and the Ser285 hydroxy group. Non-bonded interactions were found between the ligand and Tyr7, Thr8, Ser9, Tyr45, Ala95, Val112, His113, Tyr190, Asp262, Lys271, His281, Lys282, Ser285, Glu288 and Phe292. For non-cyclam **1**, the binding conformation showed two side chain hydrogen bond donors between the non-cyclam protonated secondary amine and the Glu288 oxygen and the other non-cyclam protonated secondary amine and the Ser285 oxygen. Non-bonded interactions were found between the ligand and Ile6, Tyr7, Thr8, Ser9, Phe36, Leu41, Ala95, Val112, His113, Asn176, Arg188, Tyr190, Tyr255, Ser285 and Glu288. Finally, for bicyclam AMD3100, a side chain hydrogen bond donor was found between the cyclam ring protonated N11 and the Ser285 oxygen and two ionic interactions between the cyclam ring N1 and the Glu288 oxygen and the opposite cyclam ring protonated N11 and the Glu288 oxygen. Non-bonded interactions were found between the ligand and Ile6, Tyr7, Thr8, Arg30, Phe36, Cis109, Val112, His113, Asn176, Arg188, Tyr190, Tyr255, Lys282, Ile284, Ser285 and Glu288.

Although these are the first molecular modeling ligand interaction studies for **1**, **2** and **3**, it is interesting to note that the binding interactions of AMD3100, AMD3465 and AMD3451 described here agree with those from previous reports.[16,22,26,30]

None of the dockings into CXCR4 (even refined by MD) are capable of explaining all mutant results by a direct ligand-receptor interaction. That is to say, none of the binding modes obtained could account for all of the amino acid residues that have been shown to affect the binding of the well-known CXCR4 bicyclam and monocyclam inhibitors.[16,22,26,30] To accommodate all the amino acid residues indicated by the mutational analysis it is necessary to explore different high-affinity

docking binding modes for each molecule. However, in all binding modes obtained there appear interactions with Glu288 and Asp262, which agree with the CXCR4 SDM residues with the highest level of the effect of the mutation on the binding of well-known monocyclam and bicyclam compounds. This result is consistent with the work of Wong et al.,[30] who propose two possible explanations for this fact: one explanation is that there are indeed amino acid residues that interact with small-molecule inhibitors over a longer distance and the other is that small-molecule inhibitors can bind in several orientations to the receptor by directly interacting with different subsets of amino acid residues, the results of mutagenesis reflecting a timed average.

Conclusions

In conclusion, novel monocyclam derivatives have been designed, synthesized, and biologically evaluated as HIV entry inhibitors. In vitro activity testing of these compounds in cell cultures against HIV strains has displayed EC_{50} values of 0.02 and 0.06 $\mu g\,mL^{-1}$ without cytotoxicity at the tested concentrations. Furthermore, the specificity of these monocyclams for CXCR4 has been proven by staining studies of mAbs against CXCR4, CD4 and CD45. Docking and MD simulations have been performed to predict the binding interactions between CXCR4 and the novel monocyclam derivatives. A binding mode of these compounds has been proposed which is consistent with the CXCR4 SDM residues with the highest level of the effect of the mutation on the binding of well-known monocyclam compounds such as AMD3465, AMD3529, AMD8721, AMD8899 or AMD3389. Moreover, docking and MD comparisons have been performed between monocyclams (the novel monocyclams reported herein, as well as other published monocyclam compounds), non-cyclams (non-cyclam compounds previously reported by our group, from which derive the monocyclams, as well as published non-cyclams), and bicyclams (the well known AMD3100 bicyclam). Our results suggest that these three structurally diverse CXCR4 inhibitors, monocyclams (**2** and **3**), non-cyclams (compound **1**) and bicyclams (AMD3100) bind to overlapping but not identical amino acid residues in the transmembrane regions of the receptor. Therefore, these new monocyclams might serve as novel leads for further pharmacological investigations as therapeutic agents against HIV.

Experimental Section

Chemistry

General methods: IR spectra were recorded in a Nicolet Magna 560 FTIR spectrophotometer. ^1H and ^{13}C NMR spectra were recorded in a Varian Gemini-300 operating at a field strength of 300 and 75.5 MHz, respectively, and Varian 400-MR operating at a field strength of 400 and 100.6 MHz, respectively. Chemical shifts (δ) are reported in parts per million (ppm), and coupling constants (J) in Hz using, in the case of ^1H NMR, TMS or TSPNa as an internal standard and setting, in the case of ^{13}C NMR the reference at the signal of the solvent, 77.0 ppm ($CDCl_3$). Standard and peak multiplicities are designated as follows: s, singlet; d, doublet; t, triplet; q, quartet; m, multiplet; br, broad signal; cs, complex signal. Mass spectra (*m/z* (%), EI, 70 eV) were obtained using a Hewlett–Packard HP5988A spectrometer and Bruker Biotof spectrometer (ESI). Elemental microanalyses were obtained on a Carlo–Erba CHNS-O/EA 1108 and EuroVector EuroEA3000 analyzers. Thin-layer chromatography (TLC) was performed on pre-coated sheets of silica 60 Polygram SIL N-HR/UV254 (Macherey–Nagel, 804023). Flash chromatography was performed using silica gel 35–70 μm (SDS, 2000027). Compounds **9**, **10**,[21] and **12**[20] were synthesized by previously described methods.

1-[4-(Carboxaldehyde)phenylmethyl]-4,8,11-tris-(*tert*-butoxycarbonyl)-1,4,8,11-tetraazacyclotetradecane (5): A solution of **10** (1.22 g, 2.4 mmol) in MeCN (25 mL) was added to a mixture of **12** (0.49 g, 2.4 mmol) and K_2CO_3 (0.67 g, 4.8 mmol) in MeCN (25 mL). The mixture was held at reflux for 16 h. It was then cooled to room temperature, and the solids were filtered off. The solvent was removed under reduced pressure, and the residue was purified by column chromatography (CH_2Cl_2/MeOH) to give **5** (1.33 g, 89%) as a white solid. ^1H NMR (300 MHz, $CDCl_3$): $\delta = 9.99$ (s, 1H), 7.82 (d, $J = 8.0$ Hz, 2H), 7.45 (d, $J = 8.0$ Hz, 2H), 3.61 (s, 2H), 3.30 (m, 12H), 2.63 (br, 2H), 2.39 (br, 2H), 1.90 (br, 2H), 1.69 (m, 2H), 1.47 (s, 18H), 1.43 ppm (s, 9H); ^{13}C NMR (75.5 MHz, $CDCl_3$): $\delta = 191.7$, 155.4, 146.4, 135.3, 129.6, 129.4, 79.7, 79.6, 59.7, 53.3, 51.9, 47.8, 47.2, 46.2, 28.6, 28.5, 27.1 ppm; IR (film): $\nu = 3004$, 2975, 2932, 2870, 2817, 1695, 1607, 1478, 1465, 1390, 1366, 1247, 1165, 859 cm^{-1}; MS (IE, 70 eV): *m/z* (%): 619.7 (5), 618.7 (14) $[M]^+$; Anal. calcd for $C_{33}H_{54}N_4O_7$: C 64.05, H 8.80, N 9.05, O 18.10, found: C 64.04, H 8.77, N 8.93.

1-[4-(3-(2-Methylpiperidin-1-yl)propyl-1-aminomethyl)phenylmethyl]-4,8,11-tris-(*tert*-butoxycarbonyl)-1,4,8,11-tetraazacyclotetradecane (13): $Ti(OiPr)_4$ (1.19 g, 4.0 mmol) was added to a solution of **5** (1.26 g, 2.0 mmol) and **6** (0.33 g, 2.0 mmol) in absolute EtOH (30 mL). The mixture was stirred at room temperature for 36 h. Then $NaBH_4$ (0.08 g, 2.0 mmol) was added, and the mixture was stirred at room temperature overnight. H_2O (20 mL) was added, and the solids were filtered off. The product was extracted with CH_2Cl_2, dried over $MgSO_4$, and the solvent was removed under reduced pressure. The residue was purified by column chromatography (CH_2Cl_2/MeOH) to give **13** (1.17 g, 76%) as a yellow oil. ^1H NMR (400 MHz, $CDCl_3$): $\delta = 7.22$ (m, 4H), 3.75 (s, 2H), 3.52 (s, 2H), 3.34–2.23 (m, 12H), 2.87 (m, 1H), 2.73 (m, 1H), 2.64 (t, $J = 6.9$ Hz, 2H), 2.62 (br, 2H), 2.37 (m, 3H), 2.26 (m, 2H), 2.11 (m, 1H), 1.90 (br, 2H), 1.73–1.59 (m, 9H), 1.67 (br, 2H), 1.47 (s, 18H), 1.44 (s, 9H), 1.28 (m, 2H), 1.05 ppm (d, $J = 6.3$ Hz, 6H); ^{13}C NMR (100.6 MHz, $CDCl_3$): $\delta = 155.8$, 139.3, 137.5, 129.4, 128.2, 79.8, 79.6, 59.7, 56.2, 54.0, 53.2, 52.5, 52.3, 51.5, 48.6, 47.6–46.1, 34.9, 31.1, 28.7, 26.4, 26.0, 24.2, 19.3 ppm; IR (film): $\nu = 2974$, 2931, 2804, 1690, 1477, 1465, 1413, 1366, 1166, 754 cm^{-1}; MS (ESI): *m/z* (%): 759.6 $[M]^+$; Anal. calcd for $C_{42}H_{74}N_6O_6$: C 66.46, H 9.83, N 11.07, O 12.65, found: C 66.47, H 10.26, N 10.93.

1-[4-(3-Morpholinopropyl-1-aminomethyl)phenylmethyl]-4,8,11-tris-(*tert*-butoxycarbonyl)-1,4,8,11-tetraazacyclotetradecane (14): Compound **5** (1.26 g, 2.0 mmol) and **7** (0.44 g, 3.0 mmol) were dissolved in MeOH (15 mL) in a microwave vessel, Na_2SO_4 was added, and the vessel was sealed. The mixture was heated for 3 h at 100 °C in the microwave. Then it was filtered, diluted with MeOH, cooled to 0 °C and treated with $NaBH_4$ (0.08 g, 2.0 mmol) and stirred at room temperature overnight. H_2O (20 mL) was then added, and the product was extracted with CH_2Cl_2. The organic layers were combined, washed with brine, dried over $MgSO_4$, and the solvent was removed under reduced pressure. The residue was purified by column chromatography (CH_2Cl_2/MeOH) to give **14**

(0.48 g, 32%) as a yellow oil. ^{1}H NMR (300 MHz, $CDCl_3$): $\delta = 7.29$ (m, 4H), 3.86 (s, 2H), 3.65 (t, $J = 4.5$ Hz, 4H), 3.53 (s, 2H), 3.34–2.25 (m, 12H), 2.84 (t, $J = 6.5$ Hz, 2H), 2.62 (br, 1H), 2.46 (m, 6H), 2.37 (br, 2H), 1.89 (br, 2H), 1.83 (t, $J = 6.5$ Hz, 2H), 1.67 (br, 2H), 1.47 (s, 18H), 1.44 ppm (s, 9H); ^{13}C NMR (75.5 MHz, $CDCl_3$): $\delta = 155.4$, 137.6, 129.1, 127.9, 79.6, 79.4, 66.9, 59.4, 57.5, 53.7, 53.4, 51.3, 48.0, 47.3, 45.9, 29.7, 28.5, 26.0 ppm; IR (film): $\nu = 2971$, 2927, 2853, 2808, 1693, 1477,1464, 1365, 1165 cm^{-1}.

1-[4-(3-(2-Methylpiperidin-1-yl)propyl-1-aminomethyl)phenylmethyl]-1,4,8,11-tetraazacyclotetradecane hexahydrochloride (2): HCl (1 M in Et_2O, 18 mL) was added to **13** (1.07 g, 1.4 mmol) and stirred at room temperature overnight. Then the solvent was removed under reduced pressure to give **2** (1.03 g, 90%) as a white solid. ^{1}H NMR (400 MHz, D_2O): $\delta = 7.51$ (m, 4H), 4.38 (s, 2H), 4.21 (s, 2H), 3.51 (br, 8H), 3.41 (m, 1H), 3.30 (br, 9H), 3.09 (m, 4H), 2.91 (m, 1H), 2.17–1.99 (br, 6H), 1.86 (m, 2H), 1.71 (m, 1H), 1.59 (m, 1H), 1.44 (m, 2H), 1.24 (d, $^3J_{H,H} = 6.4$ Hz, 3H); ^{13}C NMR (100.6 MHz, D_2O): $\delta = 132.9$, 132.0, 131.1, 130.6, 60.3, 58.7, 56.8, 52.6, 50.9, 49.6, 48.3, 48.0, 44.9, 44.5, 42.0, 41.4, 38.1–37.6, 31.7, 23.2, 21.6, 20.3, 18.5, 17.4 ppm; IR (film): $\nu = 2953$, 2749, 2678, 1624, 1581, 1455 cm^{-1}; MS (ESI): m/z (%) = 459.4 (100) $[M+H]^+$; Anal. calcd for $C_{27}H_{50}N_6 \cdot 6HCl \cdot 7^1/_2 H_2O$: C 39.89, H 8.82, N 10.33, O 14.76, Cl 20.20, found: C 39.91, H 8.41, N 10.00.

1-[4-(3-Morpholinopropyl-1-aminomethyl)phenylmethyl]-1,4,8,11-tetraazacyclotetradecane hexahydrochloride (3): HCl (1 M in Et_2O, 8 mL) was added to **14** (0.46 g, 0.6 mmol) and stirred at room temperature overnight. The solvent was then removed under reduced pressure, and the solid was recrystallized from MeOH to give **3** (0.16 g, 37%) as a white solid. ^{1}H NMR (300 MHz, D_2O): $\delta = 7.59$ (m, 4H), 4.36 (br, 2H), 4.33 (br, 2H), 4.16 (br, 2H), 4.11 (br, 2H), 3.83 (m, 2H), 3.59–3.55 (m, 10H), 3.37–3.19 (m, 14H), 2.28–2.09 ppm (m, 6H); ^{13}C NMR (75.5 MHz, D_2O): $\delta = 132.5$, 132.0, 131.2, 64.3, 58.1, 56.2, 54.3, 52.2, 51.4, 50.3, 48.7, 46.9, 44.7, 43.2, 40.0, 21.1, 20.0 ppm; IR (KBr): $\nu = 2958$, 2787, 1583, 1472, 1440, 1107, 772 cm^{-1}; MS (ESI): m/z (%): 447.38 (100) $[M+H]^+$; Anal. calcd for $C_{25}H_{46}N_6O \cdot 6HCl \cdot 3H_2O$: C 41.71, H 8.14, N 11.67, O 8.89, Cl 29.59, found: C 41.57, H 7.99, N 11.44.

Docking studies

Docking studies were performed using the AutoDock Vina program.[31] This version of AutoDock uses, as input files, the 3D coordinates of both ligand and receptor, which must be converted into the appropriate format by using the ADT program.[32] The 3D structure of the CXCR4 receptor was first homology modeled with Modeller[35] and Congen[36] by using bovine rhodopsin as a template[37] as described in Pérez-Nueno et al.[38] Ligand structures were built, assigned Gasteiger partial charges,[39] and minimized in MOE with the MMFF94x force field.[33] Finally, the CXCR4 homology model and the different ligand structures were prepared for docking experiments using the ADT program. For the ligands, non-polar hydrogen atoms were deleted, and rotatable bonds were defined. For the protein, non-polar hydrogen atoms were deleted and charges were added to the structure. Both structures were saved in the appropriated format to be used with AutoDock. A cubic grid of 20 Å on each side (1 Å grid spacing) was used and was centered on the CXCR4 SDM-defined binding pocket.[24] 100 independent Lamarckian genetic algorithm (LGA) runs were performed and pseudo-Solis and Wets minimization methods were applied by using default parameters. Exhaustiveness was set to 8 and energy_range was set to 4. Key SDM residues[40–42] in the receptor binding pocket were allowed to be flexible.

Molecular dynamics simulations

The highest-affinity binding conformation obtained for each ligand (**1**, **2**, **3**, AMD3100) in the docking studies was used as the starting structure for MD simulations. Ligand structures were parameterized using the program Antechamber and the general Amber force field (gaff.dat).[43] The topology and starting coordinates of CXCR4 receptor with each of the ligands in the binding cavity were prepared using Leap. The complexes were immersed in a box of water molecules (TIP3PBOX) and Cl^- counterions were added to the solvent bulk of the protein/water complexes to maintain neutrality of the system using the program Amber 8.[34] Periodic boundary conditions were applied. The Amber force field ff03[44] all atom parameters (parm99.dat + frcmod.ff03) were used for the protein and Cl^- ions. The minimization protocol consisted of two steps: min1 and min2. Min1 consisted of 200 cycles of steepest descent followed by 4800 cycles of conjugate gradient method until the root-mean square deviation (RMSD) of the Cartesian elements of the gradient reached a value < 0.1 Å. Restraints on all protein atoms were applied (force constant of 50 kcal mol^{-1} Å^{-2}). The min2 step used the same minimization parameters but no restraints were applied, all the system was minimized. The dynamic protocol consisted of five steps: MD1, MD2, MD3, MD4, and MD5. The initial temperature for MD1 was set at 50 K, and for MD2, MD3, MD4, and MD5 were set at 300 K, while the targeted temperature during the run was 300 K. The Langevin equilibration scheme,[45] with a collision frequency value of 0.1 ps^{-1}, was applied to keep the temperature constant. The time step for all five dynamic procedures was 0.002 ps. For minimization and MD, the primary cutoff distance for non bonded interaction was set at 8 Å. In all five dynamic steps, the Shake algorithm[46] was applied to constrain only bonds involving hydrogen and omit force evaluations for these bonds. Regarding the MD protocol used, the first step (MD1) aimed for the equilibration of water molecules and ions of the water-boxed and charge-neutralized the model. An initial velocity was given to the system and trajectories were then allowed to evolve in time according to Newtonian laws, keeping the protein model fixed (restraints on all protein atoms with a force constant of 25 kcal mol^{-1} Å^{-2}). The number of dynamics steps was 20000, corresponding to 40 ps. Periodic boundary dynamic, with constant volume and no pressure control, was performed on the system. In the second step (MD2), 40 ps of constant pressure dynamic of 1 atm, with isotropic position scaling, was applied with restraints on all protein atoms (force constant of 10 kcal mol^{-1} Å^{-2}). In the subsequent steps (MD3, MD4, MD5), 40 ps of constant pressure dynamic of 1 atm were also applied with restraints on backbone atoms, applying force constants of 10, 5, and 1 kcal mol^{-1} Å^{-2}, respectively, to finally assess the stability of the models over time.

Antiviral activity evaluations

The reference HIV-1 NL4–3 strain was titered in MT-4 cells after acute infection, and infectivity was measured by evaluating the cytopathic effect induced after 5 day cultures as described.[47,48] Anti-HIV activity (EC_{50}) and cytotoxicity (CC_{50}) measurements in MT-4 cells were based on viability of cells that had been infected or not infected with HIV-1, all exposed to various concentrations of the test compound. After the MT-4 cells were allowed to proliferate for five days, the number of viable cells was quantified by a tetrazolium-based colorimetric method (MTT method). Values represent the mean ± standard deviation of at least two independent evaluations done in triplicate.

Flow cytometry analysis

Staining of chemokine receptor CXCR4, CD45, and CD4 receptor on MT-4 cell line was performed as reported previously.[48,49] Briefly, 0.1×10^6 cells were washed in PBS and then they were incubated for 20 min at room temperature with mAbs anti-CD45 conjugated with fluorescein isothiocyanate at 1:200 dilution, 12G5 (anti-CXCR4)-phycoerythrin (PE) at 1:50 dilution and Leu3a (anti-CD4)-peridin chlorophyll protein at 1:50 dilution (BD Biosciences, San Jose, CA, USA), and with or without study drugs and control compounds (AMD3100 and unstained 12G5). The cells were then washed with PBS and fixed in PBS containing 1% formaldehyde. Cells were analyzed by flow cytometry in a FacsCalibur system (BD Biosciences). Data were acquired and analyzed with CellQuest software (BD Biosciences). AMD3100, Leu3a, 12G5 and the study drugs were tested at various concentrations. The compound concentration required to inhibit mAb binding by 50% (IC_{50}) was calculated from the percent mean inhibition results from three independent experiments.

Acknowledgements

This work was supported in part by the Fundació Marató de TV3 project 020930 and the Spanish Ministerio de Educación y Ciencia project SAF-2007-6322 (J.I.B. and B.C.) and BFU-2009-06958 (J.A.E.). M.P.M. holds a research fellowship from FIS. V.I.P.-N. held a 2008FI scholarship from Generalitat de Catalunya, and S.P. from IQS.

Keywords: CXCR4 antagonists · docking · HIV-1 infection · medicinal chemistry · molecular dynamics

[1] UNAIDS, AIDS Epidemic Update: December 2007, http://www.unaids.org/en/KnowledgeCentre/HIVData/EpiUpdate/EpiUpdArchive/2007/default.asp (accessed May 11, 2010).
[2] J. A. Esté, A. Telenti, *Lancet* **2007**, *370*, 81 – 88.
[3] N. J. Anthony, *Curr. Top. Med. Chem.* **2004**, *4*, 979 – 990.
[4] I. Markovic, K. A. Clouse, *Curr. HIV Res.* **2004**, *2*, 223 – 234.
[5] J. A. Esté, T. Cihlar, *Antiviral Res.* **2010**, *85*, 25 – 33.
[6] E. De Clercq, *Med. Chem. Res.* **2004**, *14*, 439 – 478.
[7] E. De Clercq, *Expert Opin. Emerging Drugs* **2005**, *10*, 241 – 274.
[8] W. M. Kazmierski, J. P. Peckman, M. Duan, T. P. Kenakin, S. Jenkinson, K. S. Gudmundsson, S. C. Piscitelli, P. L. Feldman, *Curr. Med. Chem. Anti-Cancer Agents* **2005**, *4*, 133 – 152.
[9] K. de Vresse, D. Reymen, P. Griffin, A. Stinkasserer, G. Werner, G. J. Bridger, J. A. Esté, W. James, G. W. Henson, J. Desmyter, J. Anne, E. De Clercq, *Antiviral Res.* **1996**, *29*, 209 – 219.
[10] D. Schols, J. A. Esté, G. Henson, E. De Clercq, *Antiviral Res.* **1997**, *35*, 147 – 156.
[11] E. De Clercq, *Mol. Pharmacol.* **2000**, *57*, 833 – 839.
[12] J. A. Esté, C. Cabrera, E. De Clercq, S. Struyf, J. van Damme, G. Bridger, R. T. Skerlj, M. J. Abrams, G. Henson, A. Gutiérrez, B. Clotet, D. Schols, *Mol. Pharmacol.* **1999**, *55*, 67 – 73.
[13] S. Hatse, K. Princen, E. De Clercq, M. M. Rosenkilde, T. W. Schwartz, P. E. Hernandez-Abad, R. T. Skerlj, G. J. Bridger, D. Schols, *Biochem. Pharmacol.* **2005**, *70*, 752 – 761.
[14] K. Princen, S. Hatse, K. Vermiere, S. Aquaro, E. De Clercq, L.-O. Gerlach, M. Rosenkilde, T. W. Schwartz, R. Skerlj, G. Bridger, D. Schols, *J. Virol.* **2004**, *78*, 12996 – 13006.
[15] N. D. Stone, S. B. Dunaway, C. Flexner, C. Tierney, G. B. Calandra, S. Becker, Y.-J. Cao, I. P. Wiggins, J. Conley, R. T. MacFarland, J.-G. Park, C. Lalama, S. Snyder, B. Kallungal, K. L. Klingman, C. W. Hendrix, *Antimicrob. Agents Chemother.* **2007**, *51*, 2351 – 2358.
[16] M. M. Rosenkilde, L.-O. Gerlach, S. Hatse, R. T. Skerlj, D. Schols, G. J. Bridger, T. W. Schwartz, *J. Biol. Chem.* **2007**, *282*, 27354 – 27365.
[17] S. Pettersson, V. I. Pérez-Nueno, L. Ros-Blanco, R. Puig de La Bellacasa, M. O. Rabal, X. Batllori, B. Clotet, I. Clotet-Codina, M. Armand-Ugón, J. A. Esté, J. I. Borrell, J. Teixidó, *ChemMedChem* **2008**, *3*, 1549 – 1557.
[18] V. I. Pérez-Nueno, S. Pettersson, D. W. Ritchie, J. I. Borrell, J. Teixidó, *J. Chem. Inf. Model.* **2009**, *49*, 810 – 823.
[19] J. I. Luengo, A. T. Price, A. Shaw, K. Wiggall, World Patent WO 00/66112 (filing date: May 3, 2000).
[20] C. Schickaneder, F. W. Heinemann, R. Alsfasser, *Eur. J. Inorg. Chem.* **2006**, 2357 – 2363.
[21] E. Kawabata, K. Kikuchi, Y. Urano, H. Kojima, A. Odani, T. Nagano, *J. Am. Chem. Soc.* **2005**, *127*, 818 – 819.
[22] L.-O. Gerlach, R. Skerlj, G. Bridger, T. W. Schwartz, *J. Biol. Chem.* **2001**, *276*, 14153 – 14160.
[23] W. B. Zhang, J. M. Navenot, B. Haribabu, H. Tamamura, K. Hiramatu, A. Omagari, G. Pei, J. P. Manfredi, N. Fujii, J. R. Broach, S. C. A. Peiper, *J. Biol. Chem.* **2002**, *277*, 24515 – 24521.
[24] A. Brelot, N. Heveker, M. Montes, M. J. Alizon, *J. Biol. Chem.* **2000**, *275*, 23736 – 23744.
[25] G. A. Donzella, D. Schols, S. W. Lin, J. A. Esté, K. A. Nagashima, P. J. Maddon, G. P. Allaway, T. P. Sakmar, G. Henson, E. De Clercq, J. P. Moore, *Nat. Med.* **1998**, *4*, 72 – 77.
[26] S. Hatse, K. Princen, L.-O. Gerlach, G. Bridger, G. Henson, E. De Clercq, T. W. Schwartz, D. Schols, *Mol. Pharmacol.* **2001**, *60*, 164 – 173.
[27] S. Hatse, K. Princen, K. Vermeire, L.-O. Gerlach, M. M. Rosenkilde, T. W. Schwartz, G. Bridger, E. De Clercq, D. Schols, *FEBS Lett.* **2003**, *546*, 300 – 306.
[28] S. N. Ho, H. D. Hunt, R. M. Horton, J. K. Pullen, L. R. Pease, *Gene* **1989**, *77*, 51 – 59.
[29] M. M. Rosenkilde, L.-O. Gerlach, J. S. Jacobsen, R. T. Skerlj, G. J. Bridger, T. W. Schwartz, *J. Biol. Chem.* **2004**, *279*, 3033 – 3041.
[30] R. S. Y. Wong, V. Bodart, M. Metz, J. Labrecque, G. Bridger, S. P. Fricker, *Mol. Pharmacol.* **2008**, *74*, 1485 – 1495.
[31] O. Trott, A. J. Olson, *J. Comput. Chem.* **2009**, *31*, 455 – 461; http://vina.scripps.edu (accessed May 11, 2010).
[32] The Scripps Research Institute, MGL Tools, http://mgltools.scripps.edu (accessed May 11, 2010).
[33] MOE: Molecular Operating Environment, Chemical Computing Group Inc., Montreal, QC (Canada), 2006.
[34] D. A. Case, T. A. Darden, T. E. Cheatham III, C. L. Simmerling, J. Wang, R. E. Duke, R. Luo, K. M. Merz, B. Wang, D. A. Pearlman, M. Crowley, S. Brozell, V. Tsui, H. Gohlke, J. Mongan, V. Hornak, G. Cui, P. Beroza, C. Schafmeister, J. W. Caldwell, W. S. Ross, P. A. Kollman, Amber 8, University of California, San Francisco, 2004, http://amber.scripps.edu (accessed May 11, 2010).
[35] A. Sali, T. L. Blundell, *J. Mol. Biol.* **1993**, *234*, 779 – 815.
[36] R. E. Bruccoleri, *Mol. Simul.* **1993**, *10*, 151 – 174.
[37] C. Seibert, T. P. Sakmar, *Curr. Pharm. Des.* **2004**, *10*, 2041 – 2062.
[38] V. I. Pérez-Nueno, D. W. Ritchie, O. Rabal, R. Pascual, J. I. Borrell, J. Teixidó, *J. Chem. Inf. Model.* **2008**, *48*, 509 – 533.
[39] J. Gasteiger, M. Marsili, *Tetrahedron* **1980**, *36*, 3219 – 3228.
[40] C. Bissantz, G. Folkers, D. Rognan, *J. Med. Chem.* **2000**, *43*, 4759 – 4767.
[41] H. Gutiérrez-de-Terán, M. Pastor, N. B. Centeno, J. Aqvist, F. Sanz, *ChemBioChem* **2004**, *5*, 841 – 849.
[42] X. Huang, J. Shen, M. Cui, L. Shen, X. Luo, K. Ling, G. Pei, H. Jiang, K. Chen, *Biophys. J.* **2003**, *84*, 171 – 184.
[43] J. M. Wang, R. M. Wolf, J. W. Caldwell, P. A. Kollamn, D. A. Case, *J. Comput. Chem.* **2004**, *25*, 1157 – 1174.
[44] Y. Duan, C. Wu, S. Chowdhury, M. C. Lee, G. Xiong, W. Zhang, R. Yang, P. Cieplak, R. Luo, T. Lee, J. Caldwell, J. Wang, P. Kollman, *J. Comput. Chem.* **2003**, *24*, 1999 – 2012.
[45] R. W. Pastor, B. R. Brooks, A. Szabo, *Mol. Phys.* **1998**, *65*, 1409 – 1419.
[46] J.-P. Ryckaert, G. Ciccotti, H. J. C. Berendsen, *J. Comput. Phys.* **1977**, *23*, 327 – 341.
[47] G. Moncunill, M. Armand-Ugón, E. Pauls, B. Clotet, J. A. Esté, *AIDS* **2008**, *22*, 23 – 31.
[48] G. Moncunill, M. Armand-Ugón, I. Clotet-Codina, E. Pauls, E. Ballana, A. Llano, B. Romagnoli, J. W. Vrijbloed, F. O. Gombert, B. Clotet, S. De Marco, J. A. Esté, *Mol. Pharmacol.* **2008**, *73*, 1264 – 1273.
[49] E. Ballana, E. Pauls, J. Senserrich, B. Clotet, F. Perron-Sierra, G. C. Tucker, J. A. Esté, *Blood* **2009**, *113*, 1278 – 1286.

[50] G. J. Bridger, R. T. Skerlj, P. E. Hernandez-Abad, D. E. Bogucki, Z. Wang, Y. Zhou, S. Nan, E. M. Boehringer, T. Wilson, J. Crawford, M. Metz, S. Hatse, K. Princen, E. De Clercq, D. Shols, *J. Med. Chem.* **2010**, *53*, 1250 – 1260.
[51] It is common in the pharmaceutical industry to have assays that generate IC_{50} or EC_{50} values rather than equilibrium constants. Whereas pK_i and ΔG form a strict linear correlation [$\Delta G = RT\ln(K)$], the correlation between pEC_{50} and ΔG cannot be expected to be exactly linear. However, IC_{50} or EC_{50} values can be used to obtain ΔG in an approximate manner, as in: R. Zhou, R. A. Friesner, A. Ghosh, R. C. Rizzo, W. L. Jorgensen, R. M. Levy, *J. Phys. Chem. B* **2001**, *105*, 10388 – 10397.
[52] Scoring functions can calculate $\Delta G_{binding}$ values with low computational cost, predicting free energy values in good qualitative agreement with experiment; see: R. Wang, Y. Lu, S. Wang, *J. Med. Chem.* **2003**, *46*, 2287 – 2303. Approaches based on MD such as LIE (see: J. Åqvist, C. Medina, J. E. Samuelson, *J. Protein Eng.* **1994**, *7*, 385 – 391) or MM-PBSA (see: J. Srinivasan, T. E. Cheatham, P. Cieplak, P. A. Kollman, D. A. Case, *J. Am. Chem. Soc.* **1998**, *120*, 9401 – 9409) allow predictions that are reliable and in good agreement with experiment, but are much more computationally expensive. The results obtained using AutoDock Vina affinity scoring function are impressive due to the good agreement with experimental values obtained.

Received: March 25, 2010
Revised: April 29, 2010
Published online on June 8, 2010

